Available online at www.sciencedirect.com
ScienceDirect
Bioorganic & Medicinal Chemistry 15 (2007) 656–662
Bioorganic & Medicinal Chemistry

Discovery of *Helicobacter pylori* shikimate kinase inhibitors: Bioassay and molecular modeling

Cong Han,[a,†] Jian Zhang,[a,†] Lili Chen,[a] Kaixian Chen,[a] Xu Shen[a,b,*] and Hualiang Jiang[a,b,*]

[a]*Drug Discovery and Design Center, State Key Laboratory of Drug Research, Shanghai Institute of Materia Medica, Shanghai Institutes for Biological Sciences, Chinese Academy of Sciences, Shanghai 201203, China*
[b]*School of Pharmacy, East China University of Science and Technology, Shanghai 200237, China*

Received 2 October 2006; revised 26 October 2006; accepted 28 October 2006
Available online 1 November 2006

Abstract—Shikimate kinase (SK) is the fifth enzyme in the shikimate pathway and catalyzes the phosphate transfer from ATP to shikimate in generating shikimate 3-phosphate and ADP. SK has been developed as a promising target for the discovery of antibacterial agents. In this report, two small molecular inhibitors (compound **1**, 3-methoxy-4-{[2-({2-methoxy-4-[(4-oxo-2-thioxo-1,3-thiazolidin-5-ylidene)methyl]phenoxy}methyl)benzyl]oxy}benzaldehyde; compound **2**, 5-bromo-2-(5-{[1-(3,4-dichlorophenyl)-3,5-dioxo-4-pyrazolidinylidene]methyl}-2-furyl)benzoic acid) against *Helicobacter pylori* SK (HpSK) were successfully identified with IC_{50} values of 5.5 ± 1.2 and 6.4 ± 0.4 μM, respectively. The inhibition kinetics shows that compound **1** is a noncompetitive inhibitor with respect to both shikimate and MgATP, and compound **2** is a competitive inhibitor toward shikimate and noncompetitive inhibitor with respect to MgATP. The surface plasmon resonance (SPR) technology based analysis reveals that the equilibrium dissociation constants (K_Ds) of compounds **1** and **2** with HpSK enzyme are 4.39 and 3.74 μM, respectively. The molecular modeling and docking of two inhibitors with HpSK reveals that the active site of HpSK is rather roomy and deep, forming an L-shape channel on the surface of the protein, and compound **1** prefers the corner area of L-shape channel, while compound **2** binds the short arm of the channel of SK in the binding interactions. It is expected that our current work might supply useful information for the development of novel SK inhibitors.

1. Introduction

Since *Helicobacter pylori* was discovered by Marshall and Warren in 1982,[1] the rapid infection of *H. pylori* has been a severe threat to human health. Colonization of human stomach by *H. pylori* is a major causative factor for gastrointestinal illnesses such as chronic gastritis, peptic ulcer, and gastric cancer.[2] So far, *H. pylori* has been recognized to chronically infect the stomachs of up to 50% of the world's human population. Currently, combination therapies employing one proton pump inhibitor (e.g., omeprazole) and two or three antibiotics (e.g., metronidazole, amoxicillin, and clarithromycin) have been used as preferred treatments.[3] However, the multiple therapy regiments have not been very effective in clinical setting, because the overuse and misuse of antibacterial agents has resulted in the emergence of antibiotic-resistant strains.[4] Therefore, there are urgent needs to discover novel anti-*H. pylori* agents. Accordingly, it is obviously necessary to identify new molecular targets to develop new drugs against the pathogen.

In bacteria, the shikimate pathway is essential for the synthesis of important metabolites such as aromatic amino acids, folic acid, and ubiquinone.[5] Because the shikimate pathway is crucial to algae, higher plants, bacteria, and fungi, but absent from mammals,[6,7] the enzymes involved in the pathway have been considered potential drug targets for developing nontoxic antimicrobial agents, herbicides, and antiparasite

Abbreviations: SK, shikimate kinase; NMP, nucleoside monophosphate; SB, shikimate-binding; SPR, surface plasmon resonance; IPTG, isopropyl-β-D-thiogalactopyranoside; PK, pyruvate kinase; LDH, lactate dehydrogenase; RU, response unit.

Keywords: Shikimate kinase; *Helicobacter pylori*; Enzyme inhibitor; Surface plasmon resonance; Molecular modeling.

* Corresponding authors. Tel./fax: +86 21 50806918 (X.S.); e-mail addresses: xshen@mail.shcnc.ac.cn; hljiang@mail.shcnc.ac.cn
† Both authors contributed equally to this work.

0968-0896/$ - see front matter © 2006 Elsevier Ltd. All rights reserved.
doi:10.1016/j.bmc.2006.10.058

drugs.[8] In the shikimate pathway, shikimate kinase (SK, EC 2.7.1.71) is the fifth enzyme that catalyzes a phosphate transfer from ATP to shikimate, producing shikimate 3-phosphate and ADP.[9] In *Escherichia coli*, the SK reaction is catalyzed by two different isoforms, SK I and SK II, which are encoded by *aroK* gene and *aroL* gene, respectively. The physiological function of SK I is not clear in *E. coli*, while the SK II appears to play a pivotal role.[10] Conversely, the complete genome sequence of *H. pylori* has revealed the presence of only SK I enzyme that plays an essential role in the shikimate pathway.

The three-dimensional structures of SKs from *E. coli*, *H. pylori*, *Campylobacter jejuni* (PDB code 1VIA), *Erwinia chrysanthemi*, and *Mycobacterium tuberculosis*, including structures of enzyme–substrate complexes, have been discovered in the last few years.[11–14] The reported SK structures show that SK belongs to the same structural family of nucleoside monophosphate (NMP) kinases that consist of three domains: CORE, LID, and NMP-binding domains.[15] The CORE domain contains a highly conserved phosphate-binding loop (P-loop), the LID domain bears functionally essential residues to bind ATP, and the NMP-binding domain is replaced by the shikimate-binding (SB) domain in SK.

Although the functional and structural studies of SKs from several different bacteria have provided a consolidated platform for the development of SK inhibitors, there is still few report about SK inhibitor to date. In this report, we constructed an enzymatic screening model based on *H. pylori* SK (HpSK). Using high-throughput screening against our laboratory chemical library, two potent HpSK inhibitors (compound **1** 3-methoxy-4-{[2-({2-methoxy-4-[(4-oxo-2-thioxo-1,3-thiazolidin-5-ylidene)methyl]phenoxy}methyl)benzyl]oxy}benzaldehyde and compound **2** 5-bromo-2-(5-{[1-(3,4-dichlorophenyl)-3,5-dioxo-4-pyrazolidinylidene]methyl}-2-furyl)benzoic acid) were successfully identified with IC_{50} values of micromole activities. To the best of our knowledge, our finding is the first report about SK inhibitor to date. Furthermore, to validate the inhibition mechanisms of the inhibitors and find clues for designing new inhibitors, the binding interactions and affinities of the two inhibitors with HpSK were also performed by molecular modeling and surface plasmon resonance (SPR) technology.

2. Results

2.1. High-throughput screening against our chemical library to identify HpSK inhibitor

The recombinant HpSK was cloned, expressed, and purified in *E. coli* system. A double coupled assay involving pyruvate kinase (PK) and lactate dehydrogenase (LDH) was used to evaluate HpSK enzyme activity. According to the enzyme assay procedure, a high-throughput screening against our chemical library of 3000 compounds was performed to identify potent HpSK inhibitors. Compounds **1** and **2** were identified as HpSK inhibitors, yielding IC_{50} values of 5.5 ± 1.2 and 6.4 ± 0.4 μM, respectively. The chemical structures of compounds **1** and **2** are shown in Figure 1. Figure 2 depicts the dose-dependent inhibition of HpSK by compounds **1** and **2**. As shown in Figure 2, HpSK enzyme activity gradually decreased with the increased concentrations of compound **1**, while HpSK enzyme activity sharply decreased when the concentration of compound **2** was changed from 1 to 50 μM. In a separate control experiment under the same conditions lack of HpSK enzyme, compounds **1** and **2** cannot inhibit PK and LDH activities at concentrations up to 20 μM, which thereby further confirms that compounds **1** and **2** are indeed HpSK inhibitors. Since there is no any report about SK inhibitor to date, our discovery will no doubt supply some useful information for the development of novel SK inhibitors.

2.2. Inhibition modes of HpSK inhibitors

The inhibition kinetics was conducted to determine the inhibition modes of compounds **1** and **2**. The data collected at varied substrate and inhibitor concentrations yielded a series of intersecting lines when plotted as a double-reciprocal plot. Figure 3 shows the inhibition kinetics of HpSK enzyme with respect to shikimate and MgATP in the presence of compound **1**, which indicates that compound **1** is a noncompetitive inhibitor with respect to shikimate (or MgATP) as fitted to the noncompetitive inhibition equation (Eq. 1), where K_i is the dissociation constant for the inhibitor–enzyme complex, and αK_i is the dissociation constant for the inhibitor–enzyme–substrate complex. The inhibition kinetics of HpSK enzyme toward shikimate in the presence of compound **2** is shown in Figure 4A, which illustrates that compound **2** serves as a competitive inhibitor with respect to shikimate, fitting to the competitive inhibition equation (Eq. 2). Figure 4B reveals the inhibition kinetics of HpSK enzyme toward MgATP in the presence of compound **2**, which demonstrates that compound **2** is a noncompetitive inhibitor with respect to MgATP, fitting to the noncompetitive inhibition equation (Eq. 1). Table 1 summarizes the kinetic inhibition data of compounds **1** and **2**.

$$v = \frac{V_{\max}[S]}{[S]\left(1 + \frac{[I]}{\alpha K_i}\right) + K_m\left(1 + \frac{[I]}{K_i}\right)} \quad (1)$$

$$v = \frac{V_{\max}[S]}{[S] + K_m\left(1 + \frac{[I]}{K_i}\right)} \quad (2)$$

2.3. Binding affinity of inhibitor with HpSK

SPR analysis provides insight into the association and dissociation kinetics of the interaction between inhibitor and enzyme. Various concentrations of samples were increased from 0 to 50 μM for kinetic analysis. The binding responses in response unit (RU) were continuously recorded and presented graphically as a function of time (Fig. 5), clearly presenting the association and

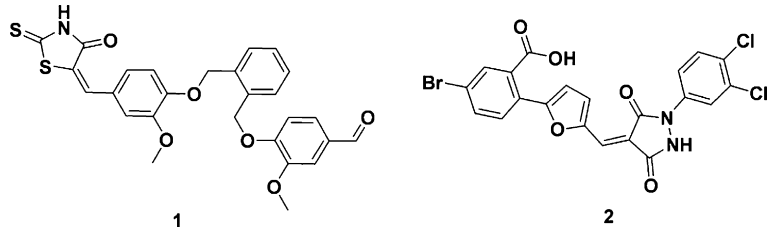

Figure 1. The chemical structures of compounds **1** and **2**.

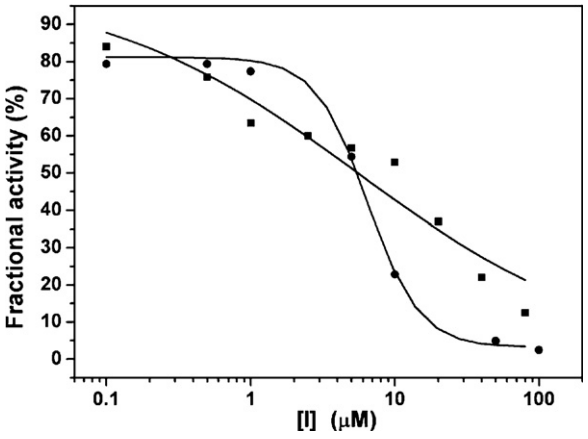

Figure 2. The dose-dependent inhibition of HpSK by compounds **1** and **2**. compound **1** (■), compound **2** (●).

dissociation phases of the binding reaction. The kinetic analysis was fitted to a 1:1 (Langmuir) binding model, yielding k_a (the association rate constant), k_d (the dissociation rate constant), and K_D (the equilibrium dissociation constant, $K_D = k_d/k_a$) values of 791 M^{-1} s^{-1}, 3.47×10^{-3} s^{-1}, and 4.39 μM for compound **1**, and k_a, k_d, and K_D values of 1340 M^{-1} s^{-1}, 5.02×10^{-3} s^{-1}, and 3.74 μM for compound **2**, respectively.

2.4. Molecular modeling of inhibitors with HpSK

To validate the inhibition mechanisms of the inhibitors and, further, find new clues for designing new inhibitors, the interaction models of these two compounds with HpSK were analyzed based on the docking simulations.

As shown in Figure 6A and B, the binding site of HpSK is rather roomy and deep, forming an L-shape channel on the surface of the protein, which is mainly composed of three sub-pockets: the short arm, the long arm, and the corner of the L-shape channel. Most of the residues in the channel are conserved in bacterial SKs. According to the crystal structures of HpSK (PDB code 1ZUH) and HpSK-shikimate-phosphate complex (PDB code 1ZUI), the short arm and the long arm of the L-shape channel are binding sites for shikimate and MgATP, respectively (Fig. 6A and B). After its binding to SK, MgATP could transfer its terminal phosphate to shikimate at the corner of the L-shape channel. For compounds **1** and **2**, the distinct binding models were discovered based on the conformations with the lowest binding free energy. Compound **1** prefers the corner area of the L-shape channel (Fig. 6A), which is stabilized by the hydrogen bondings with Gly11 and Thr78 as well as interactions with several conserved hydrophobic residues including Met10, Met34, Val44, Phe48, and Gly79 (Fig. 6C). These two hydrogen bonds fix the aldehyde group and methoxy group of the left benzene ring

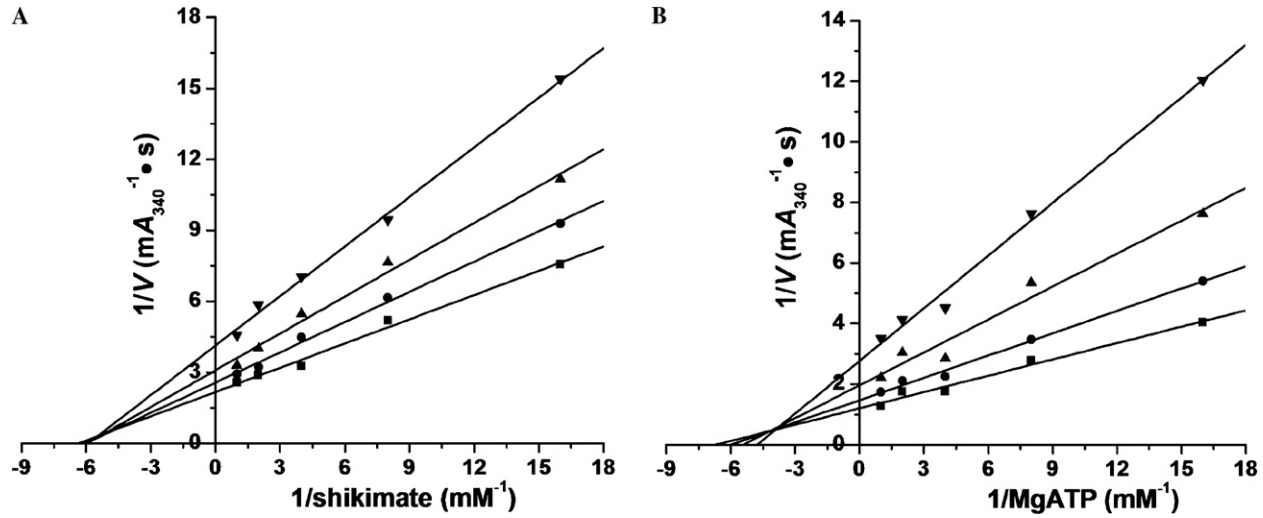

Figure 3. Lineweaver-Burk plots for inhibition of HpSK by increasing concentrations of compound **1** (0 μM (■), 2.5 μM (●), 5 μM (▲), and 10 μM (▼)) with respect to shikimate (A) and MgATP (B).

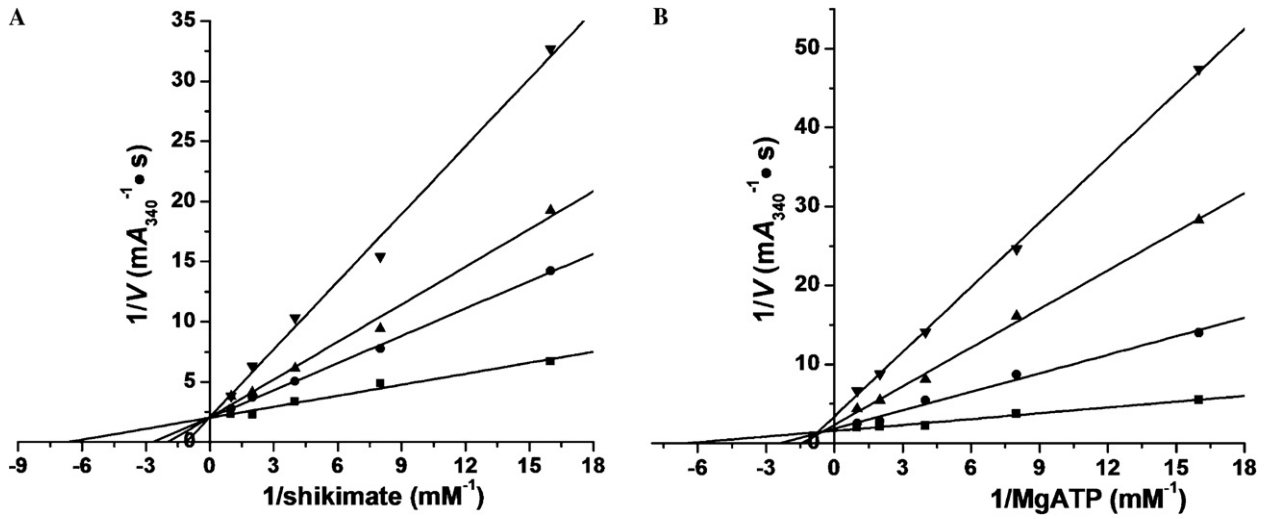

Figure 4. Lineweaver-Burk plots for inhibition of HpSK by increasing concentrations of compound **2** (0 μM (■), 2.5 μM (●), 5 μM (▲), and 10 μM (▼)) with respect to shikimate (A) and MgATP (B).

Table 1. Kinetic inhibition data of the inhibitors against HpSK enzyme

Compound	Inhibition mode		K_i (μM)	$\alpha K_{ishikimate}$ (μM)	αK_{iMgATP} (μM)
	Shikimate	MgATP			
1	Noncompetitive	Noncompetitive	9.48	10.67	7.18
2	Competitive	Noncompetitive	2.19	—	7.92

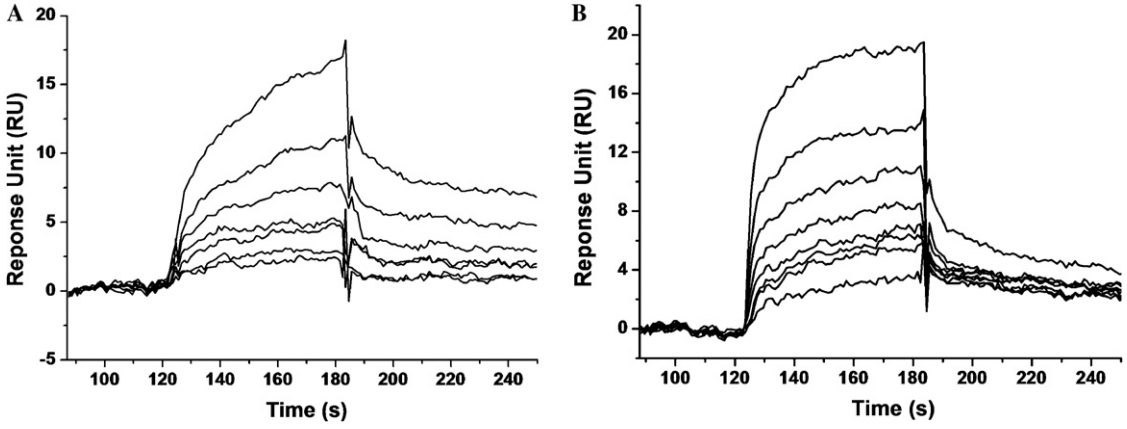

Figure 5. Binding of inhibitor to HpSK measured by SPR. (A) Biosensorgrams obtained with compound **1** at concentrations of 35, 24.5, 17.15, 12, 8.4, 5.88, and 4.12 μM. (B) Biosensorgrams obtained with compound **2** at concentrations of 50, 35, 24.5, 17.15, 12, 8.4, 5.88, and 4.12 μM.

of compound **1** at the corner of the channel (Fig. 6C), and the hydrophobic residues contribute desolvation energy to the tight binding. However, compound **2** binds the short arm of the channel (Fig. 6B). The salt bond between Arg124 and the carboxyl group of the right benzene ring of compound **2** is the key interaction for positioning compound **2** to the short arm (Fig. 6D). Besides the salt bond, the hydrophobic environment of the short arm of L-shape channel, composed of Phe9, Met10, Phe48, Gly79, Gly80, Gly81, Ile82, Phe101, Ile105, Leu108, Glu114, Leu120, and Phe121, provides a good place to accommodate the rest of compound **2** (Fig. 6D).

3. Discussion

In recent years, the shikimate-pathway enzymes, serving as novel drug–targets, have received more attention from pharmaceutical companies. A wide variety of inhibitors have been developed to block the growth of plants and microorganisms. For example, the compound glyphosate produced by Monsanto company, the inhibitor of 5-enoylpyruvyl shikimate phosphate synthase, was proved to be one of the world's best-selling herbicides and inhibit the growth of apicomplexan parasites in vitro.[7] The compound 6(*S*)-fluoroshikimate produced by AstraZeneca company is converted to

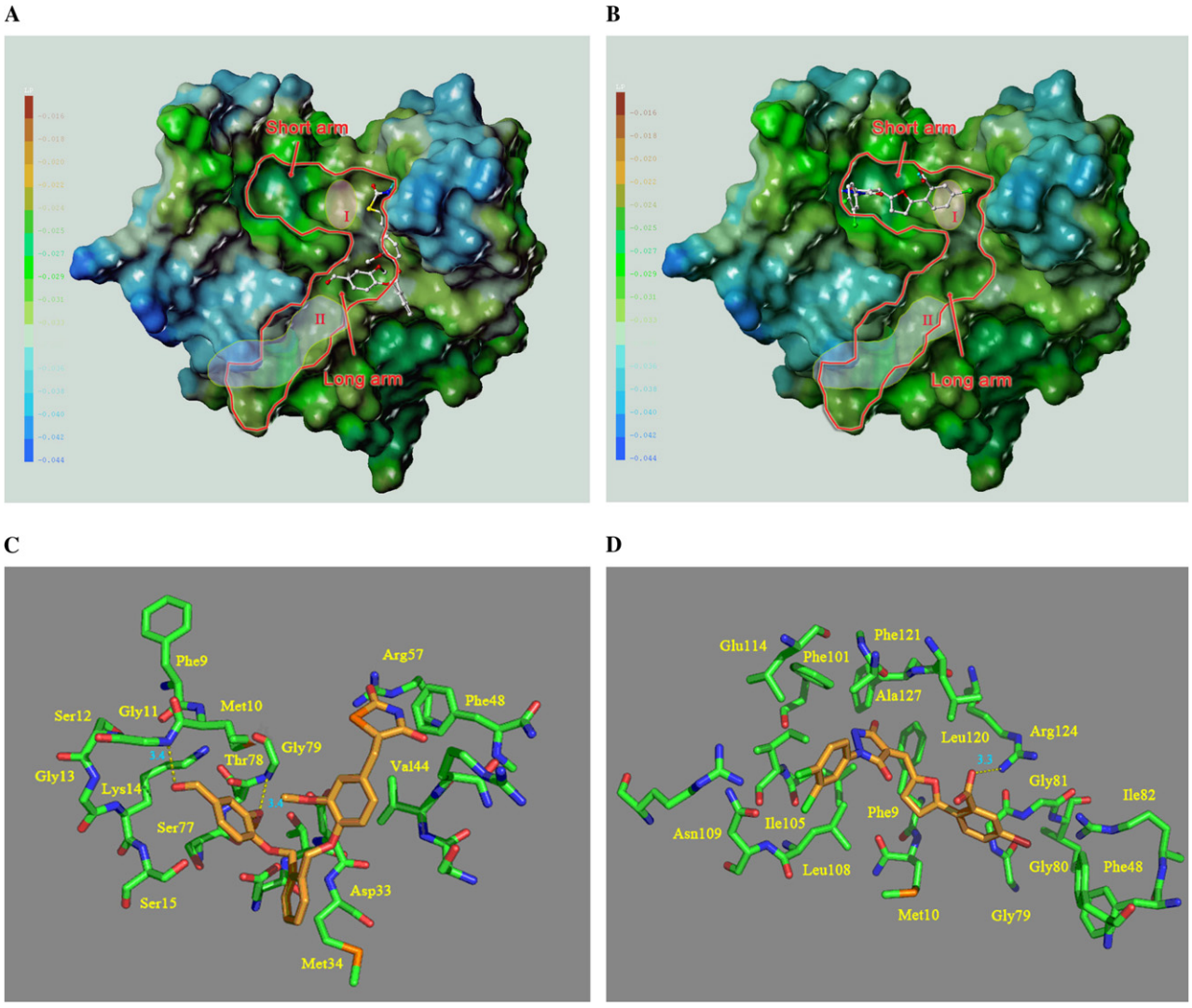

Figure 6. Binding models of compounds **1** and **2** to HpSK. Compound **1** (A) and compound **2** (B) were docked into the binding pocket of HpSK. The compounds are displayed in stick mode with atom type colors. Area I and II represent the binding sites for shikimate and MgATP, respectively. The binding interactions of compounds **1** (C) and **2** (D) are shown in stick mode. The hydrogen bonds and salt bond are represented by yellow dash lines and blue labels.

6-fluorochorismate by the subsequent enzymes in the shikimate pathway. 6(*S*)-Fluoroshikimate could block the biosynthesis of *p*-aminobenzoic acid and inhibit the growth of *E. coli*.[16,17] These findings suggest that the inhibitors targeting the shikimate pathway are promising antimicrobial agents.

Compounds **1** and **2** were identified as HpSK inhibitors by high-throughput screening. The enzymatic inhibition kinetics demonstrates that compound **1** is a noncompetitive inhibitor with respect to both shikimate and MgATP, and compound **2** acts as a competitive inhibitor toward shikimate and noncompetitive inhibitor with respect to MgATP. The bioassay experiments indicate that the binding site for compound **1** to HpSK enzyme is different from that for compound **2**. On the other hand, the molecular modeling studies of the inhibitors with HpSK also show two different binding models about the inhibitors. Compound **1** binds to the corner sub-pocket, which has no effect on the binding of either shikimate or MgATP, but can block the phosphate transfer from MgATP to shikimate. Compound **2** binds to the short arm of the L-shape channel to preclude shikimate from binding HpSK. The molecular modeling features are in good agreement with the inhibition kinetics results. Furthermore, the hydrogen bond plays a dominating role in the interaction between compound **1** and HpSK, while the salt bond makes a great contribution to the binding of compound **2** to HpSK. Our binding models provide insight into specific interactions involved in the potential inhibitors as well as a new clue to study the inhibition mechanism of HpSK inhibitors.

SPR is a rapid and sensitive method for evaluating the affinities and the elementary steps involved in bimolecular interactions. According to our SPR assays, the K_D value of compound **1** is higher than that of compound **2**, which demonstrates that the binding affinity of compound **2** to HpSK is more potent than that of compound **1**. In parallel, K_i value of compound **1** is almost

3-fold higher than that of compound **2**, which also proves the above conclusion from SPR assay.

In summary, we have constructed a high-throughput screening platform for HpSK inhibitor. Compounds **1** and **2** were identified as HpSK inhibitors with potent activity. The discovery of HpSK inhibitors might serve as a starting point for further chemical modification and screening to develop novel antimicrobial agents with increased specificity and potency.

4. Experimental

4.1. Materials

Helicobacter pylori strain SS1 was obtained from Shanghai Institute of Digestive Disease. *E. coli* host strain BL21(DE3) was purchased from Stratagene. The chemical library containing 3000 compounds with diverse chemical scaffolds was purchased from Specs company (http://www.specs.net). All chemicals were of reagent grade or ultra-pure quality, and commercially available.

4.2. Cloning, expression, and purification of the recombinant *H. pylori* SK

Based on the genome sequences of *H. pylori* strains 26695 and J99 (GenBank Accession Nos. NC_000915 and NC_000921), a pair of PCR primers (sense: 5′-GCGCATCCATATGCAGCATTTAGTTTTAATCG-3′ and antisense: 5′-CCGCTCGAGTGCGATGAATTGTAGCAC-3′) was synthesized to clone *aroK* gene from *H. pylori* strain SS1. The PCR products were digested with restriction endonucleases *Nde*I and *Xho*I (Takara), and cloned into a prokaryotic expression vector pET-22b (Novagen) with a C-terminal six-histidine tag for purification purpose. The nucleotide sequence of *aroK* gene from *H. pylori* strain SS1 has been deposited in the GenBank database under GenBank Accession No. AY692135.

Escherichia coli BL21(DE3) cells were transformed with the recombinant plasmid pET22b-HpSK. The transformed cells grown in LB media were induced by 0.4 mM isopropyl-β-D-thiogalactopyranoside (IPTG) and incubated at 25 °C for an additional 6 h. The cells were harvested by centrifugation and sonicated on ice. The recombinant HpSK protein was purified by immobilized-nickel ion affinity chromatography combined with Sephacryl S-100 gel filtration chromatography (Amersham Biosciences). Fractions containing HpSK were pooled and concentrated by ultrafiltration with Amicon centrifugal filter device. All the purification, dialysis, and concentration procedures were performed at 4 °C. Protein concentrations were determined by Bradford assay using bovine serum albumin as the standard.

4.3. Enzymatic activity assay

The enzymatic activity of HpSK was evaluated by using a double coupled assay involving PK and LDH.[18] During the assay, the ADP generated by SK leads to the oxidation of NADH to NAD^+. All assays at 25 °C were conducted in a 96-well plate spectrophotometer (Tecan GENios reader) by measuring the decrease in absorbance at 340 nm ($\varepsilon = 6180\ M^{-1}\ cm^{-1}$). The assay solution (total volume 200 μl) contained 100 mM Tris–HCl (pH 8.0), 50 mM KCl, 5 mM $MgCl_2$, 2 mM ATP, 2 mM phosphoenolpyruvate, 0.7 mM NADH, 3 U/ml PK, 2.5 U/ml LDH, and 2 mM shikimate. The reaction was initiated by the addition of the diluted HpSK enzyme.

4.4. Inhibitor discovery

Our laboratory chemical library containing 3000 compounds was used for screening HpSK inhibitor. Based on the procedure of enzyme activity assay, the initial velocities of the enzyme activity were determined in the presence of compounds (10 μM) dissolved in dimethylsulfoxide (Me_2SO). The final Me_2SO concentration in all assay mixtures was 0.1% (v/v). The assay buffer contained 2 mM shikimate and 2 mM ATP. The reaction was initiated by the addition of the diluted HpSK enzyme (20 nM). After the preliminary screening, compounds **1** and **2** were identified to inhibit HpSK enzyme activity in vitro. The initial velocities of the enzyme activity were determined in the presence of various concentrations of compounds **1** and **2** (0–100 μM) to investigate the dose-dependent inhibition effects. IC_{50} values of the two inhibitors were obtained by fitting the data to a sigmoid dose–response equation of the Origin software (OriginLab). Afterwards, inhibitor modality was determined by measuring the effect of inhibitor concentration on the enzymatic velocity as a function of substrate concentration. In one inhibition experiment where the ATP concentration was fixed at 2 mM (saturated concentration), shikimate was a varied substrate (0.0625, 0.125, 0.25, 0.5, and 1 mM) when the concentration of inhibitor was varied from 0 to 10 μM. In parallel, where the shikimate concentration was fixed at 2 mM (saturated concentration), ATP was a varied substrate (0.0625, 0.125, 0.25, 0.5, and 1 mM) when the concentration of inhibitor was varied from 0 to 10 μM.

4.5. SPR analysis

To further investigate the binding affinity of inhibitor with HpSK, SPR analysis based on Biacore 3000 (Biacore) was performed. Protein immobilization, binding experiments, and data analysis were addressed with the preexisting templates in the instrument's software. HpSK enzyme (10 mM sodium acetate buffer, pH 4.5, 50 μg/ml) was covalently coupled to the surface matrix of CM5 sensor chip (Biacore). Equilibration of the baseline was accomplished by a continuous flow of HBS-EP running buffer (10 mM Hepes, 150 mM NaCl, 3 mM EDTA, and 0.005% (v/v) surfactant P20, pH 7.4) through the chip for 1–2 h. Samples were automatically injected into flow cells with concentrations increased gradually. All the data were collected at 25 °C with HBS as running buffer (flow rate 30 μl/min). The k_a, k_d, and K_D values were determined by the 1:1 (Langmuir) binding fit model.

4.6. Molecular modeling and docking

The crystal structure of HpSK (PDB code 1ZUH) was recovered from Brookhaven Protein Database (http://www.rcsb.org/pdb). The missing residues from Lys111 to Leu118 were added to HpSK structure. The repaired residues were subjected to energy minimization in Sybyl 6.8 (Tripos Associates) using steepest descent method. The potential of HpSK 3D structure was assigned according to the Amber 4.0 force field with Kollman-united-atom charges encoded in Sybyl 6.8. The compounds **1** and **2** were also constructed by Sybyl 6.8. The geometries of the compounds were subsequently optimized using the MMFF94 force field,[19] MMFF94 charges, and Powell method. A nonbond cutoff of 8 Å was adopted to consider the intramolecular interaction. For the purpose of tackling the interacting mode of these two compounds with HpSK, the advanced docking program AutoDock 3.0.3 was used to perform the automated molecular docking. In the Autodock calculations, the Lamarckian genetic algorithm was applied to deal with the ligand–enzyme interactions.[20] The numbers of generation, energy evaluation, and docking runs were set to 370,000, 15,000,000, and 20, respectively. Finally, the interaction models of the compounds with HpSK were produced using the LIGPLOT program.[21]

Acknowledgments

This work was supported by the State Key Program of Basic Research of China (Grant 2004CB58905), the National Natural Science Foundation of China (Grants 30525024 and 20372069), Shanghai Basic Research Project from the Shanghai Science and Technology Commission (Grants 06JC14080, 03DZ19228) and Foundation of Chinese Academy of Sciences (Grant KSCX1-YW-R-18).

References and notes

1. Warren, J. R.; Marshall, B. J. *Lancet* **1983**, *1*, 1273–1275.
2. Cover, T. L.; Blaser, M. J. *Adv. Intern. Med.* **1996**, *41*, 85–117.
3. Ulmer, H. J.; Beckerling, A.; Gatz, G. *Helicobacter* **2003**, *8*, 95–104.
4. Cameron, E. A.; Powell, K. U.; Baldwin, L.; Jones, P.; Bell, G. D.; Williams, S. G. *J. Med. Microbiol.* **2004**, *53*, 535–538.
5. Parish, T.; Stoker, N. G. *Microbiology* **2002**, *148*, 3069–3077.
6. Kishore, G. M.; Shah, D. M. *Annu. Rev. Biochem.* **1988**, *57*, 627–663.
7. Roberts, C. W.; Johnson, J. J.; Kyle, D. E.; Krell, T.; Coggins, J. R.; Coombs, G. H.; Milhous, W. K.; Tzipori, S.; Ferguson, D. J.; Chakrabarti, D.; McLeod, R. *Nature* **1998**, *393*, 801–805.
8. Coggins, J. R.; Abell, C.; Evans, L. B.; Frederickson, M.; Robinson, D. A.; Roszak, A. W.; Lapthorn, A. P. *Biochem. Soc. Trans.* **2003**, *31*, 548–552.
9. Berlyn, M. B.; Giles, N. H. *J. Bacteriol.* **1969**, *99*, 222–230.
10. Whipp, M. J.; Pittard, A. J. *J. Bacteriol.* **1995**, *177*, 1627–1629.
11. Romanowski, M. J.; Burley, S. K. *Proteins* **2002**, *47*, 558–562.
12. Cheng, W. C.; Chang, Y. N.; Wang, W. C. *J. Bacteriol.* **2005**, *187*, 8156–8163.
13. Krell, T.; Coggins, J. R.; Lapthorn, A. J. *J. Mol. Biol.* **1998**, *278*, 983–997.
14. Gan, J.; Gu, Y.; Li, Y.; Yan, H.; Ji, X. *Biochemistry* **2006**, *45*, 8539–8545.
15. Vonrhein, C.; Schlauderer, G. J.; Schulz, G. E. *Structure* **1995**, *3*, 483–490.
16. Bornemann, S.; Ramjee, M. K.; Balasubramanian, S.; Abell, C.; Coggins, J. R.; Lowe, D. J.; Thorneley, R. N. *J. Biol. Chem.* **1995**, *270*, 22811–22815.
17. Davies, G. M.; Barrett-Bee, K. J.; Jude, D. A.; Lehan, M.; Nichols, W. W.; Pinder, P. E.; Thain, J. L.; Watkins, W. J.; Wilson, R. G. *Antimicrob. Agents Chemother.* **1994**, *38*, 403–406.
18. Krell, T.; Maclean, J.; Boam, D. J.; Cooper, A.; Resmini, M.; Brocklehurst, K.; Kelly, S. M.; Price, N. C.; Lapthorn, A. J.; Coggins, J. R. *Protein Sci.* **2001**, *10*, 1137–1149.
19. Halgren, T. *J. Am. Chem. Soc.* **1990**, *112*, 4710–4723.
20. Morris, G. M.; Goodsell, D. S.; Halliday, R. S.; Huey, R.; Hart, W. E.; Belew, R. K.; Olson, A. J. *J. Comp. Chem.* **1998**, *19*, 1639–1662.
21. Wallace, A. C.; Laskowski, R. A.; Thornton, J. M. *Protein Eng.* **1995**, *8*, 127–134.